Short communication

# Transport properties of fast proton conducting mesoporous silica xerogels

M.T. Colomer *, F. Rubio, J.R. Jurado

*Instituto de Cerámica y Vidrio, CSIC, C/Kelsen n° 5, Campus de la Universidad Autónoma, 28049 Madrid, Spain*

## Abstract

Mesoporous acid-free silica xerogels exhibiting a proton conductivity of $2.0 \times 10^{-2}$ S cm$^{-1}$ at 80 °C and 81% RH is reported for the first time. The proton conductivity values, lower cost and higher hydrophilicity of mesoporous silica xerogels make them potential substitutes for Nafion membranes in proton exchange membranes fuel cells (PEMFCs).
© 2007 Elsevier B.V. All rights reserved.

*Keywords:* Fuel cells; Proton exchange membranes; Silica xerogels; Mesoporosity

## 1. Introduction

Proton conducting materials have attracted much attention because of their potential use in clean-energy fields such as fuel cells [1], capacitors [2], proton sensors [3], and ion-exchange-membranes [1]. The series of perfluorosulfonate ionomers such as Nafion are the most well-known proton conductive materials and serve as ion-exchange membranes due to their high proton conductivity [1]. However, their conductivity decreases at temperatures higher than 80 °C because of their inability to retain water, instability at high temperature (above 100 °C) and swelling in water. They are susceptible to deformation on the basis of their repetition of ab/adsorption and desorption of water. The deformation increases interfacial resistance between the membrane and electrodes, and decreases the fuel cell performance. Furthermore, Nafion membranes are very expensive, hard to synthesize and present environmental problems with regards to recycling and disposal of fluorinated polymers and their separation from the platinum catalysts used.

Over the last 10 years, the proton conductivity characteristics of porous glasses and xerogels have been the subject of growing interest due to their potential as solid electrolytes in sensors, fuel cells, etc. [4–19]. $P_2O_5$-$SiO_2$ glasses exhibit a conductivity of $3.0 \times 10^{-2}$ S cm$^{-1}$ at 30 °C under 70% RH. However, phosphates are lacking in chemical durability since $P^{5+}$ ions are easily dissolved in water [8]. Ioroi et al. [9] prepared nanoporous $SiO_2$ glasses treated with 3-mercaptopropyltrimethoxysilane and subsequent oxidation of thiol groups to sulfonic acid groups with a proton conductivity of $1.0 \times 10^{-2}$ S cm$^{-1}$, at 40 °C and 95% RH; in this case, the detrimental problem for high temperature use of this kind of glass would be the loss of grafted $HSO_4$ branches in a similar way than Nafion [10].

Among the studied xerogels both silica and acid doped silica xerogels have been selected as potential electrolytes in proton exchange membranes fuel cells (PEMFCs) [11–19]. Up to now, the values of their proton conductivity are low in comparison with Nafion, except for those impregnated with acids or modified-silica gels. For instance, mesoporous silica gels impregnated with 5.0 M $H_2SO_4$ showed high conductivities in the order of $10^{-1}$ S cm$^{-1}$ in a temperature range from 40 to 80 °C under 60% RH [17]. However, a drastic and rapid decrease in conductivity occurs as a function of time due to a partial or total loss of the impregnated acid. When the gels are acid-free showed a proton conductivity very low ($10^{-5}$ S cm$^{-1}$) even at 80 °C and 60% RH. It may be due to the small pore size value (∼2 nm) of those gels [17].

Thus, the conductivity values of the silica xerogels must be improved without the use of acids in order to use silica films as fuel cell electrolytes. Mesoporous silica materials with an adequate pore size have several properties that may be beneficial

---

* Corresponding author. Tel.: +34 91 735 58 40; fax: +34 91 735 58 43.
  *E-mail address:* tcolomer@icv.csic.es (M.T. Colomer).

for their use as possible solid-state electrolyte alternatives. The control of pore structure such as pore diameter and pore volume of the silica gels is very important for designing the proton conducting paths [14]. It is expected that the control of the mesoporous structures leading to enhanced proton-conducting properties will contribute to the development of better proton conducting electrolytes. The sol–gel method is an excellent process for producing highly proton-conductive solid materials and the particulate sol–gel route, in particular, leads to a sharper pore size distribution in the final product.

Daiko et al. [19] reported that in the porous glasses with pores larger than ∼15 nm (diameter), the pores are not filled with the water molecules, resulting into the decreased proton conduction. As the pore size decreases, the pores are filled with the physically bonded water molecules, which act to form the pass way of proton conduction. On the other hand, in the pores smaller than ∼2 nm, most of the ad/absorbed water is chemically bound and restricts the proton hopping. A value of average pore size of 10 nm can permit the crossover that the polymeric membranes suffer [20]. Thus, an average pore size >2 and <10 nm can be the optimum value for the proton transport without crossover. As is mentioned above, the control of the pore volume is also very important to enhance the proton transport. High values of pore volume (around 0.45 g cm$^{-3}$) are desirable for a fast proton transport [14].

The objective of this work is to design mesoporous silica xerogels of high pore volume and an adequate average pore diameter (∼4.0 nm) than can retain water, with the aim of obtaining proton-exchange electrolytes for PEMFCs. A study of the electrical transport properties is reported as a function of the temperature and relative humidity.

## 2. Experimental

### 2.1. Synthesis of the SiO$_2$ xerogels

SiO$_2$ particles were prepared through sol–gel processes using tetraethyl orthosilicate (TEOS) and ammonium hydroxide or nitric acid. Starting silica sols were prepared through a TEOS/water two-phase sol–gel reaction (TEOS/water ratio: 80/1). TEOS (98% ACS reagent grade and used as received) was added to an ammonium hydroxide (0.5 M, basic hydrolysis, 30% ACS reagent grade and used as received) or nitric acid solution (10$^{-3}$ M, acid hydrolysis, 70% ACS reagent grade and used as received). The sol–gel process was started from the immiscible state and no alcohol was added. The mixture is vigorously stirred for 1 h (base catalyzed, pH 9) or overnight (acid catalyzed, pH 3) at room temperature. After hydrolysis, each mixture becomes a clear sol. The sols were put into dyalisis tubing and dialyzed against pure water to remove ammonia or nitric acid and ethanol until the pH is 9 (base hydrolysis) or 3 (acid hydrolysis). Dialysis tubing was employed to clean the sol after the hydrolysis and condensation reactions were complete (membrane tubing: Spectra/por, molecular cut-off = 3500 molecular weight). The sols prepared under acid conditions have particles with an average size of 4 nm, whereas silica particles formed at pH 9 have an average particle size of about 6 nm. A molar ratio of acid/base sols of 4.8 was employed in order to control the degree of aggregation. The xerogel was produced by drying the precursor sol under 33% RH. Dry xerogels were cleaned by double deionized water in order to eliminate the residual ions from the synthesis. Dry xerogels were fired at 300 °C in air for 1 h.

### 2.2. Textural characterization

The average particle size in the prepared sols was determined by quasi-elastic laser light scattering using photon correlation spectroscopy on a Brookhaven light scattering instrument equipped with a laser light scattering goniometer (Model BI2030AT). The wavelength of the laser light used in this instrument was 633 nm, which can detect a minimal particle size of 3 nm. X-ray diffraction analysis of the calcined xerogels were carried out with a D-5000 Siemens diffractometer using monochromatized Cu Kα radiation. The residual nitrogen content was determined on both the dried and calcined xerogels with a LECO TC-500 nitrogen analyzer, using the gas fusion method [25]. The porous structure of the xerogels was characterized by nitrogen sorption (Micromeritics ASAP 2000 poresizer) after degassing at 200 °C. N$_2$ with molecule cross-sectional area of 0.162 nm$^2$ was used as the adsorptive gas. Prior to N$_2$ sorption, all samples were degassed [(i.e. exposing the powder attained from the film to a vacuum pressure lower than 1 Pa at 200 °C overnight (20 h)]. This is done to remove physically adsorbed gases from the sample surfaces, in particular water vapor [31]. The specific surface areas were estimated in relation to the masses of the outgassed samples and calculated from the BET equation. Three isotherms were collected for each sample to ensure that the data were representative. Pore size distributions were calculated from the desorption data using the BJH method [32,33]. Pore volume was determined from the adsorption maxima. The connectivity of the membranes was calculated from the Seaton's model based on the use of the percolation theory [23].

### 2.3. Thermal analysis

Thermal analysis measurements (thermogarvimetric analysis, DTA–TG: Perkin Elmer, Model DTA7 and Model Pyris 1, respectively) were performed after the xerogels were exposed to different relative humidity (RH) at 25 °C (8, 33, 58, 75, 81 and 97%) for 24 h in sealed chambers containing saturated solutions of appropriate salts [ZnBr$_2$·2H$_2$O for 8%, MgCl$_2$·6H$_2$O for 33%, NaBr·2H$_2$O for 58%, NaCl for 75%, (NH$_4$)$_2$SO$_4$ for 81% and K$_2$SO$_4$ for 97% RH] [34] (equilibrium conditions of the samples prior to recording the DTA–TG curves). For comparison, the same type of thermal analysis was performed on a treated Nafion® 117 film. The DTA–TG curves were taken from room temperature up to 250 °C at a heating rate of 5 °C min$^{-1}$. The total water content (physisorbed and chemisorbed water) was calculated for this range of temperatures. The number of water molecules per square nanometer present in each sample is calculated from the weight loss of water at each relative humidity, calculated from TG analysis, and from the specific surface area

of each sample. In the case of Nafion the volume of the sample was taken into account for the calculation (mmol water $cm^{-3}$).

### 2.4. Electrical characterization

Electrical conductivity of the xerogels was measured by electrochemical impedance spectroscopy (EIS) using a HP-4192A frequency response analyzer. The frequency range used was $5–10^7$ Hz. Gold electrodes were sputtered prior to the electrical measurements. Before collecting impedance spectra, the xerogels were allowed to equilibrate at the desired RH (8, 33, 58, 75, 81 and 97%) for 24 h in sealed chambers containing saturated solutions of the above mentioned appropriate salts. Measurements were performed at constant temperature (from 25 to 80 °C), with the sample chamber immersed in a thermostatically controlled water bath. The reproducibility of the results was verified by repeating the measurements three times for a given sample, and also by testing different samples of the same material equilibrated under the same conditions. The spectra were fit using the EQUIVCRT program by Boukamp [35]. As the RH is controlled by using saturated salts, and the %RH for these salts depends on temperature, the conductivity for the system from 40 to 80 °C may correspond to a lower RH.

### 3. Results and discussion

#### 3.1. Textural characterization

The $N_2$ adsorption–desorption isotherm for the silica calcined xerogels is of type IV of the IUPAC classification, and exhibits an *E* hysteresis loop in accordance with de Boer [21] or type H2 from IUPAC classification [22] (Fig. 1). The width of the hysteresis is indicative of the interconnectivity of the pores. Interconnection between pores is indispensable for achieving high proton conductivity. The wider the hysteresis, the more interconnected are the pores. The value of the connectivity is $z = 4.2$ according to the Seaton's model [23] indicating an open framework with an interconnected internal structure.

The membranes were mesoporous, with a BET surface area of $534 \pm 2 \, m^2 \, g^{-1}$, average pore diameter of 3.7 nm (desorption)] (Fig. 2) and a pore volume of $0.45 \pm 0.01 \, cm^3 \, g^{-1}$. The XRD patterns of the xerogels calcined at 300 °C for 1 h correspond to amorphous materials. In order to evaluate if all the $HNO_3$ acid or
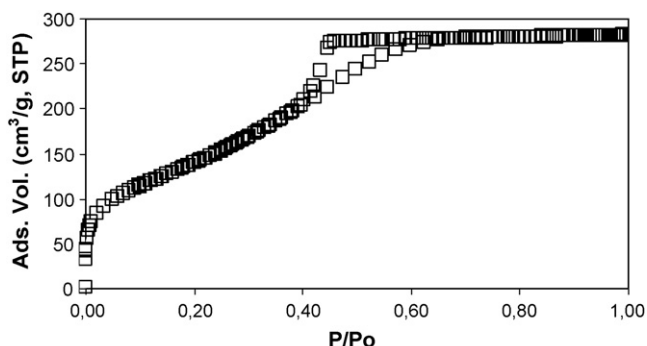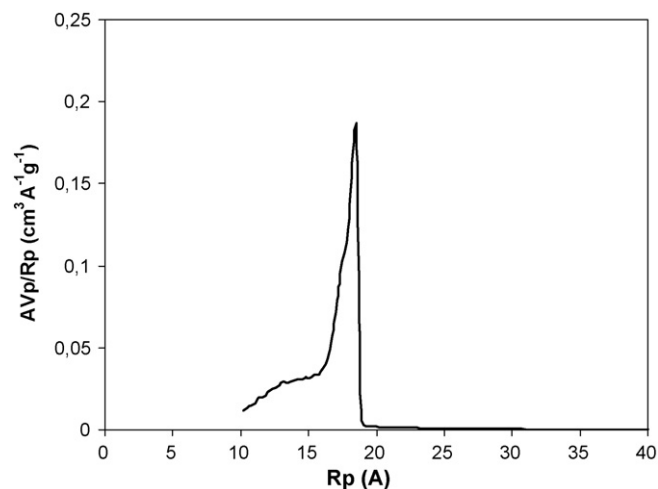


Fig. 2. Pore size distribution of the calcined silica xerogel.

ammonium hydroxide used for the synthesis are removed from the xerogels, since they can modify the proton conductivity values, a nitrogen analysis was carried out. The nitrogen analysis by the gas fusion method [25] show the presence of residual nitrogen ($0.40 \pm 0.03$ wt.%) in the uncalcined xerogels, however, no nitrogen is detected in the calcined xerogels.

#### 3.2. Thermal analysis

The xerogel adsorbs and absorbs water when exposed to certain humidity. The extent of this ad/absorption depends on the relative humidity of the atmosphere that this material experiences. The amount of adsorbed and absorbed water increases when the RH increases for the silica xerogels. The weight loss before 100 °C is assigned to physisorbed water, and the loss between 100 and 250 °C to surface hydroxyl groups and/or coordinated $H_2O$. Data extracted from the DTA curves provide evidence that the thermal stability of the physisorbed water is higher for the silica xerogel (minimum of the DTA curve: 95 °C) and lower for Nafion (89 °C) (Fig. 3).

However, it may be more relevant to this study to determine the number of water molecules per unit of specific surface area. These calculations show that, at 81% RH and 25 °C, the number



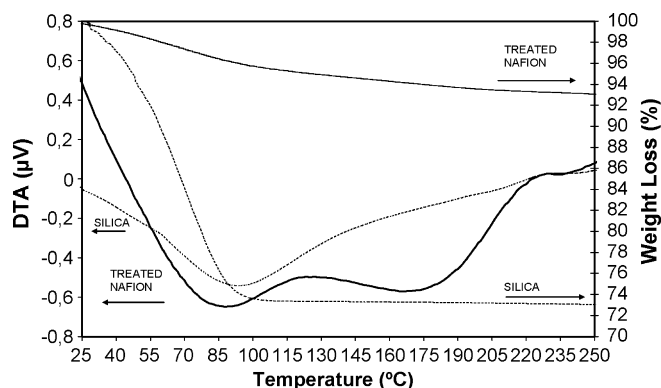Fig. 1. Nitrogen adsorption–desorption isotherm of the calcined silica xerogel.



Fig. 3. DTA and TGA curves for treated Nafion and the calcined silica xerogel, both previously equilibrated at 81% RH.

Table 1
Number of water molecules per nm$^2$ (internal specific surface area) as a function of RH

| RH (%) | Molecules nm$^{-2}$ |
|--------|---------------------|
| 8      | 2                   |
| 33     | 4                   |
| 58     | 15                  |
| 75     | 22                  |
| 81     | 24                  |
| 97     | 24                  |



Fig. 5. Proton conductivity vs. the reciprocal of the temperature at different RH for the silica xerogels.

of water molecules per square nanometer is 24 molecules nm$^{-2}$ (see Table 1) for the silica xerogels. It is difficult to describe the hydration state of Nafion using this expression because its morphology changes with the degree of hydration [24]. There is, however, literature data expressing the state of hydration of Nafion in terms of mmol water cm$^{-3}$. This value permits a more direct comparison with the silica xerogel. Under the above mentioned experimental conditions the silica xerogel showed 24 mmol cm$^{-3}$ versus 8 mmol cm$^{-3}$ for Nafion.

Fig. 4 shows the total water density as a function of the RH (water content at room temperature versus different RH in the xerogels hydrated at 25 °C). The amount of water increases significantly as the RH is increased up to 75%. After this value, the amount of water increases very slightly for higher RH. This means than this sample is almost fully water saturated in atmospheres with RH superior to 75%. For higher RH the number of molecules per nm$^2$ is the same and equal to 24 molecules nm$^{-2}$ indicating a saturation effect as a consequence of the water ad/absorption sigmoidal trend.

### 3.3. Electrical characterization

Fig. 4 also shows the proton conductivity values at 30 °C measured at different RH values. The dependence of the conductivity has also a sigmoidal trend, and according to the classification of proton conductors as a function of the water vapour partial pressure proposed by Colomban and Novak [26], the behavior of the silica xerogels is somewhere
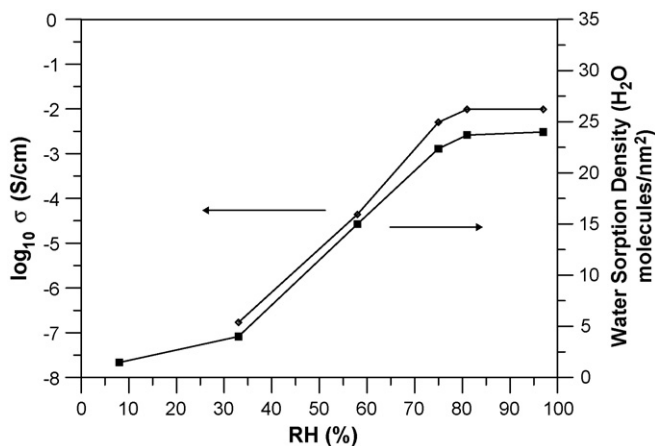


Fig. 4. Proton conductivity values at 30 °C and water content in the calcined xerogels hydrated at 25 °C vs. different RH values.
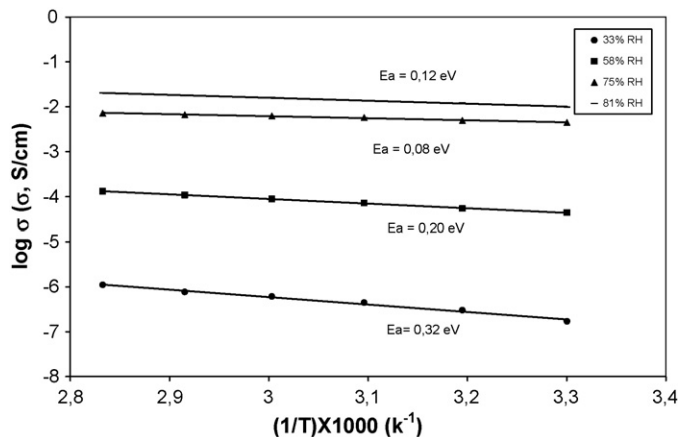
between an intrinsic conductor (bulk conductor) and a surface conductor. The data show that the conductivity increases with RH, with the greatest increase observed between 58 and 81% RH. The conductivity improves almost four orders of magnitude from 33 to 81%. The change in conductivity is from $1.7 \times 10^{-7}$ S cm$^{-1}$ at 33% RH ($\log_{10} \sigma = -6.8$) to $4.4 \times 10^{-5}$ S cm$^{-1}$ at 58% RH ($\log_{10} \sigma = -4.4$) for lower RH and exhibits a sharp change (from $4.4 \times 10^{-5}$ S cm$^{-1}$ at 58% RH ($\log_{10} \sigma = -4.4$) to $9.8 \times 10^{-3}$ S cm$^{-1}$ at 81 and 97% RH ($\log_{10} \sigma = -2.0$) at high RH. The water content increases from 4 molecules nm$^{-2}$ for 33% RH to 24 molecules nm$^{-2}$ for 81% RH. This could testify that the uptake of ad/absorbed water is a two-regime process. This mechanism of water ad/absorption was proposed by Dubinin and Serpinsky (D.S. theory) [27]. At lower RH, the water forms a layer of clusters along the walls of a matrix of interconnected pores. At higher RH, new water molecules start filling the remaining pore space through capillary condensation, and a saturation effect is observed at ~81% RH. The sharp increase in conductivity takes place over the same range of RH than that of the water content (Fig. 4).

Fig. 5 depicts the proton conductivity of the SiO$_2$ xerogels at different relative humidities versus the reciprocal of temperature (from 25 to 80 °C). An Arrhenius-like dependence with temperature is observed in all cases. At 80 °C and 81% RH, the proton conductivity is $2.0 \times 10^{-2}$ S cm$^{-1}$. The values of the activation energy ($E_a$) were obtained by linear regression of the Arrhenius equation $\sigma = \sigma_0 \exp(-E_a/KT)$, where $\sigma_0$ is a pre-exponential parameter and $K$ is the Boltzmann's constant. The activation energy values for each relative humidity are registered in Fig. 5. According to those values, proton migration is dominated by the Grotthuss mechanism. In this mechanism, the proton forms a H$_3$O$^+$ ion and jumps to the neighboring lone pair of electrons of a water molecule. For such a mechanism, the activation energy for proton conduction should be about 0.14–0.40 eV [26]. The decrease in the activation energies when relative humidity increases (up to 75% RH) can be explained from the higher water content. The filling up of channels by water molecules leads to higher conductivity, not only via the $\sigma_0$ factor, which is proportional to the number of mobile species, but also by increasing the dynamical disorder [28].

Following Sumner et al. [29] and Zawodzinski and Gottesfeld [30], the conductivity of Nafion does not depend as strongly on relative humidity as our silica xerogels. At room temperature, the values reported by Sumner et al. [29] range from $1 \times 10^{-2}$ S cm$^{-1}$ at 45% RH to $4 \times 10^{-2}$ S cm$^{-1}$ at 70% RH. At higher temperatures, the conductivity does not increase at the same rate as it does with RH, and the value reported for Nafion at 79 °C and 42% RH is $1.3 \times 10^{-2}$ S cm$^{-1}$. Furthermore, Zawodzinski and Gottesfeld [30] reported that the water content in Nafion, in terms of water molecules per sulfonate group, does not change significantly when the temperature is raised from 30 to 80 °C in samples equilibrated with water vapor, and that the membranes takes up less water as the temperature is raised. We therefore assume that the same behavior can be expected under higher temperature and RH conditions. If we extrapolate Sumner's data to the same conditions used in our study, we find that the conductivity of Nafion is about $3.7 \times 10^{-2}$ S cm$^{-1}$. Conclusively, the proton conductivity values, environmental friendly behavior, lower cost and higher hydrophilicity of nanoporous silica xerogels make them potential substitutes for Nafion membranes in proton exchange membrane fuel cells.

## 4. Concluding remarks

In summary, the silica xerogels synthesized have a high pore volume and average pore size of 3.7 nm. Proton conductivity showed a pronounced dependence on RH, with the greatest increase observed between 58 and 81% and an Arrhenius-like dependence on temperature is observed in all the RH range. The highest value of proton conductivity was found to be $2.0 \times 10^{-2}$ S cm$^{-1}$ at 80 °C and 81% RH. According to the activation energy values, proton migration is dominated by the Grotthuss mechanism in the whole range of RH.

Conclusively, nanoporous silica xerogels could be potential substitutes for Nafion membranes. Furthermore, our materials can be easily obtained as 0.5 μm thin supported films, whereas Nafion membranes are about 160 μm thick. Therefore, the actual ohmic resistance of such films would be lower than that of Nafion, in a given device.

## References

[1] K.D. Kreuer, Solid State Ionics 97 (1997) 1.
[2] P. Staiti, M. Minutoli, F. Lufrano, Electrochem. Acta 47 (2002) 2795.
[3] R. Moos, R. Müller, C. Plog, A. Knezevic, H. Leye, E. Irion, T. Braun, K. Maquardt, K. Binder, Sens. Actuators B: Chem. 83 (2002) 181.
[4] M. Nogami, Y. Abe, Phys. Rev. B 5 (1997) 12108.
[5] M. Nogami, R. Nagao, C. Wong, J. Phys.Chem. B. 102 (1998) 5772.
[6] Y. Daiko, T. Kasuga, M. Nogami, Chem. Mater. 14 (2002) 4624.
[7] Y. Abe, M. Hayashi, T. Iwamoto, H. Sumi, L.L. Hench, J. Non-Cryst. Solids 351 (2005) 2138.
[8] M. Nogami, Y. Goto, Y. Tsurita, T. Kasuga, J. Am. Ceram. Soc. 84 (2001) 2553.
[9] T. Ioroi, K. Kuraoka, K. Yasuda, T. Yazawa, Y. Miyazaki, Electrochem. Solid State Lett. 7 (2004) A394.
[10] A. Gruger, A. Régis, T. Schmatko, Ph. Colomban, Vib. Spectrosc. 26 (2001) 215.
[11] U.B. Mioc, S.K. Milonjic, D. Malovic, V. Stamenkovic, Ph. Colomban, M.M. Mitrovic, R. Dimitrijevic, Solid State Ionics 97 (1997) 239.
[12] F.M. Vichi, M.T. Colomer, M.A. Anderson, Electrochem. Solid State Lett. 2 (1999) 313.
[13] U.B. Mioc, S.K. Milonjic, V. Stamenkovic, M. Radojevic, Ph. Colomban, M.M. Mitrovic, R. Dimitrijevic, Solid State Ionics 125 (1999) 417.
[14] M.T. Colomer, M.A. Anderson, J. Non-Cryst. Solids 290 (2001) 93.
[15] A. Matsuda, T. Kanzaki, K. Tadanaga, M. Tatsumisago, T. Minami, Electrochim. Acta 47 (2001) 939.
[16] H. Li, M. Nogami, Adv. Mater. 14 (2002) 912.
[17] A. Matsuda, T. Kanzaki, K. Tadanaga, T. Kogure, M. Tatsumisago, T. Minami, J. Electrochem. Soc. 149 (2002) E292.
[18] A.A. Anappara, S. Rajeshkumar, P. Mukundan, P.R.S. Warrier, S. Ghosh, K.G.K. Warrier, Acta Mater. 52 (2004) 369.
[19] Y. Daiko, T. Kasuga, M. Nogami, Microporous Mesoporous Mater. 69 (2004) 149.
[20] N.W. Deluca, Y.A. Elabd, J. Polym. Sci.: Part B: Polym. Phys. 44 (2006) 2201.
[21] H.J. de Boer, in: D.H. Everett, F.S. Stone (Eds.), The Structure and Properties of Porous Materials, Butterworths, London, 1958, p. 195.
[22] S.J. Gregg, K.S.W. Sing, Adsorption, Surface Area and Porosity, Academic Press, London, 1982.
[23] N.A. Seaton, Chem. Eng. Sci. 46 (1991) 1895.
[24] F.N. Büchi, G.G. Sherer, J. Electroanal. Chem. 287 (1990) 163.
[25] A. Thomas, G. Muller, J. Eur. Ceram. Soc. 8 (1991) 163.
[26] P. Colomban, A. Novak, in: P. Colomban (Ed.), Proton Conductors, Cambridge University, Cambridge, 1992, pp. 38–55.
[27] M.M. Dubinin, W. Serpinsky, J. Colloid Interface Sci. 21 (1966) 378.
[28] K.D. Kreuer, I. Stoll, A. Rabenau, Solid State Ionics 9–10 (1983) 1061.
[29] J.J. Sumner, S.E. Creager, J.J. Ma, D.D. DesMarteau, J. Electrochem. Soc. 145 (1998) 107.
[30] T.A. Zawodzisnki Jr., S. Gottesfeld, Abstract 94, The Electrochemical Society Extended Abstracts, Toronto, Ontario, Canada, 1992. pp. 11–16.
[31] S. Lowell, J.E. Shields, Powder Surface Area and Porosity, Chapman and Hall, London, New York, 1991.
[32] K.S.W. Sing, D.H. Everett, R.A.W. Haul, L. Moscou, R.A. Pierotti, J. Rouquerol, T. Siemieniewska, Pure Appl. Chem. 57 (1985) 603.
[33] E.P. Barret, L.G. Joyney, P.P. Halenda, J. Am. Chem. Soc. 73 (1951) 373.
[34] David R. Lide (Editor-in-Chief), Handbook of Chemistry and Physics, 84th Edition, CRC Press, 2003–2004.
[35] B. Boukamp, Equivalent circuit (EQUIVCRT.PAS), University of Twente, Twente, The Netherlands, 1988-89.